Structure of spherical Yukawa clusters: A model for dust particles in dusty plasmas in an isotropic environment

Hiroo Totsuji,* Takafumi Ogawa, Chieko Totsuji, and Kenji Tsuruta
Graduate School of Science and Technology and Faculty of Engineering, Okayama University, Tsushimanaka 3-1-1, Okayama 700-8530, Japan
(Received 30 May 2005; published 14 September 2005)

The structure of spherical clusters composed of Yukawa particles is analyzed by molecular dynamics simulations and theoretical approaches as a model for dust particles in dusty plasmas in the isotropic environment. The latter condition is expected to be realized under microgravity or by active cancellation of the effect of gravity on the ground. It is found that, at low temperatures, Yukawa particles form spherical shells and, when scaled by the mean distance, the structure is almost independent of the strength of screening including the case of the Coulomb interaction. The positions and populations of shells and the conditions for the change of the number of shells are expressed by simple interpolation formulas. Shells have an approximately equal spacing close to that of triangular lattice planes in the bulk close-packed structures. It is shown that, when the cohesive energy in each shell is properly taken into account, the shell model reproduces the structure of spherical Yukawa clusters to a good accuracy.

DOI: 10.1103/PhysRevE.72.036406 PACS number(s): 52.27.Lw, 52.27.Gr, 82.70.Dd, 05.65.+b

I. INTRODUCTION

Systems of macroscopic (micron-sized) dust particles immersed in plasmas have been serving as an important example of strongly coupled systems since the discovery of dust crystals [1]. The interaction between dust particles is approximately described by the Yukawa potential and usual experiments may be regarded as observing the behavior of the Yukawa system under the influence of the gravity and other effects such as the ion flow and the thermophoretic force. Structures of dust particles are characterized by almost-uniformly spaced horizontal layers indicating that the gravity plays the main role in their formation [2,3]. It has been shown that the number of layers is determined by a competition between mutual repulsion of particles and the one-dimensional confining potential related to the balance of the gravity and the levitation [2,3].

The intrinsic properties of the Yukawa system, however, may appear when the system is free from the effect of gravity and in the isotropic environment. Recent experiments under microgravity [4,5] and those with active cancellation of the effect of gravity [6] are expected to realize such an isotropic Yukawa system. Some results of simulations on the isotropic three-dimensional Yukawa system have been given by the authors [7]. In this paper, we extensively analyze the structure of the Yukawa system by numerical simulations and theoretical methods assuming that the system is homogeneous and isotropic and free from the effect of ion flow and other forces. The results will be useful as a reference when we have to take the latter effects into account.

In Sec. II we obtain the Yukawa system in a confining potential as representing dust particles immersed in ambient plasmas. In Sec. III, the results of numerical simulations are summarized in the form of simple interpolation formulas and compared with the bulk close-packed structures. In Sec. IV, the shell model is applied and results of simulations are reproduced to a good accuracy. Conclusions are given in Sec. V.

II. DUST PARTICLES IN DUSTY PLASMAS AS CONFINED YUKAWA SYSTEM

Let us start from a system in a volume V, composed of N_d dust particles, N_e electrons, and N_i ions, which satisfies the condition of charge neutrality. When we denote the charges of dust particles, electrons, and ions by $-Qe$, $-e$, and e, respectively, the latter condition is expressed as

$$(-Qe)n_d + (-e)n_e + en_i = 0, \tag{2.1}$$

$n_d = N_d/V$, $n_e = N_e/V$, and $n_i = N_i/V$ being the densities of components. We take a statistical average over degrees of freedom related to electrons and ions in the adiabatic approximation and neglect the radius of dust particles and the effect of electron-electron, electron-ion, or ion-ion correlation. We then have a system of N_d dust particles where the interacting energy (exactly the Helmholtz free energy) is given by [8,9]

$$U_{coh} + U_{sheath}. \tag{2.2}$$

Here

$$U_{coh} = \frac{1}{2}\sum_{i\neq j}^{N_d} v(r_{ij}) - 2\pi N_d n_d \lambda^3 \frac{(Qe)^2}{\lambda}, \tag{2.3}$$

$$v(r) = \frac{(Qe)^2}{r}\exp(-r/\lambda), \tag{2.4}$$

$$U_{sheath} = -N_d \frac{1}{2}\frac{(Qe)^2}{\lambda}, \tag{2.5}$$

and

*Email address: totsuji@elec.okayama-u.ac.jp

$$\frac{1}{\lambda^2} = \frac{4\pi n_e e^2}{k_B T_e} + \frac{4\pi n_i e^2}{k_B T_i}. \tag{2.6}$$

The interaction between dust particles is described by the repulsive Yukawa potential (2.4) and the parameter λ characterizes the screening by electrons and ions with the temperatures T_e and T_i, respectively, which are usually different from that of dust particles T_d. The energy U_{sheath} is related to the formation of sheath around dust particles and is independent of configuration of dust particles. In dusty plasmas, the interaction between dust particles may be influenced by the ion flow and other causes. Our analyses based on Eq. (2.2) will serve as a reference in estimating those effects.

Let us note that, in Eq. (2.3),

$$-2\pi N_d n_d \lambda^3 \frac{(Qe)^2}{\lambda} = -N_d \frac{n_d}{2} \int d\mathbf{r} v(r) \tag{2.7}$$

and define the charge density in the system of dust particles $\rho(\mathbf{r})$ by

$$\rho(\mathbf{r}) = \sum_{i=1}^{N_d} (-Qe)\delta(\mathbf{r} - \mathbf{r}_i) + Qen_d. \tag{2.8}$$

Here the second term on the right-hand side is the contribution of electrons and ions which serves as the effective background charge for dust particles. Then we can rewrite U_{coh} into the form

$$U_{coh} = \frac{1}{2} \int \int_V d\mathbf{r} d\mathbf{r}' \frac{\exp(-|\mathbf{r} - \mathbf{r}'|/\lambda)}{|\mathbf{r} - \mathbf{r}'|} \rho(\mathbf{r})\rho(\mathbf{r}') - \sum_{i=1}^{N_d} \frac{(Qe)^2}{2} \int \int_V d\mathbf{r} d\mathbf{r}' \frac{\exp(-|\mathbf{r} - \mathbf{r}'|/\lambda)}{|\mathbf{r} - \mathbf{r}'|} \delta(\mathbf{r} - \mathbf{r}_i) \times \delta(\mathbf{r}' - \mathbf{r}_i), \tag{2.9}$$

where the subtracted term on the right-hand side is the self-interactions formally included in the first term. This expression indicates that dust particles are mutually interacting via the repulsive Yukawa potential and, at the same time, they are confined in the potential field ϕ_{ext} exerted by the second term of $\rho(\mathbf{r})$,

$$\phi_{ext}(\mathbf{r}) = -n_d(Qe)^2 \int_V d\mathbf{r}' \frac{\exp(-|\mathbf{r} - \mathbf{r}'|/\lambda)}{|\mathbf{r} - \mathbf{r}'|}. \tag{2.10}$$

The dusty plasma may expand and eventually fill a space of some shape limited by the electrodes or the wall of the experimental vessel. In what follows, we assume that our system occupies the inside of a sphere of radius R. This assumption may be appropriate for experiments under the condition of microgravity where we are free from the major source of anisotropy on earth, the gravity, and have a possibility to achieve an isotropic environment for dusty plasmas. We may also assume that the distribution of the background charge is uniform, as in Eqs. (2.3), (2.7), and (2.10), and further that it constitutes a uniformly charged sphere of radius R. In this case, the potential ϕ_{ext} is calculated as [7]

$$\phi_{ext}(r) = 4\pi n_d (Qe)^2 \lambda^2 \left[1 - \frac{\lambda}{r} \exp(-R/\lambda) \left(1 + \frac{R}{\lambda} \right) \times \sinh\left(\frac{r}{\lambda} \right) \right], \quad r < R, \tag{2.11}$$

$$= 4\pi n_d (Qe)^2 \lambda^2 \frac{\lambda}{r} \exp(-r/\lambda) \left[\frac{R}{\lambda} \cosh\left(\frac{R}{\lambda} \right) - \sinh\left(\frac{r}{\lambda} \right) \right], \quad R < r. \tag{2.12}$$

For dusty plasmas between parallel horizontal plates as is usual in experiments on earth, the distribution of the background charge and therefore the potential ϕ may have a one-dimensional nature and may be expressed in the form $\phi_{ext}(z)$ as a function of the coordinate along the direction of the gravity. The symmetry of the distribution of the background charge may be limited by the configuration of the electrodes even in the case of microgravity. The case of isotropic distribution analyzed here, however, may serve as a solid reference for these cases.

III. STRUCTURE OF SPHERICAL YUKAWA CLUSTERS

On the basis of the above discussions, we analyze the structure formation of dust particles in dusty plasmas by the molecular dynamics simulation under the isotropic condition which may be realized in the environment of microgravity [4,5] or by active cancellation of the effect of gravity [6]. Since U_{sheath} does not depend on the configuration of particles, we follow the dynamics of particles interacting via the Yukawa potential (2.4) in the external confining potential $\phi_{ext}(r)$ given by Eqs. (2.11) and (2.12).

A. Characteristic parameters

In our system of dust particles, we have three independent dimensionless parameters, the system size N_d, the strength of screening ξ defined by

$$\xi = a/\lambda, \tag{3.1}$$

and the strength of coupling Γ defined by

$$\Gamma = (Qe)^2/ak_B T_d, \tag{3.2}$$

where the mean distance a is defined by $(4\pi/3)[N_d/(4\pi R^3/3)]a^3 = 1$ or

$$a = R/N_d^{1/3}. \tag{3.3}$$

B. Formation of shell structure at low temperatures

Some snapshots of dust particle distribution are shown in Fig. 1. Here the positions of particles in the cylindrical coordinates (r, θ, z) are expressed by a projection onto the rz-plane. When the temperature is high, dust particles form a spherical cloud of approximate radius R with a diffuse boundary. With the decrease of the temperature, the bound-

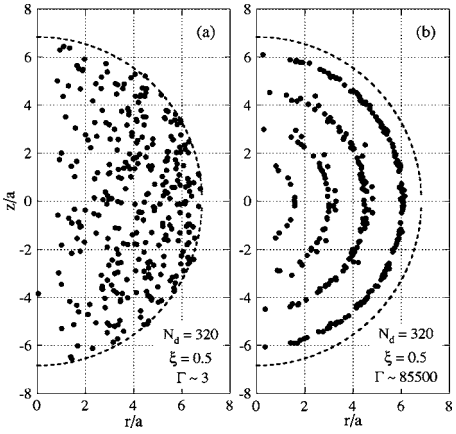

FIG. 1. Snapshots of particle distribution at high (a) and low (b) temperatures. Dotted lines correspond to $r=R$.

ary of distribution becomes sharper and eventually some shells are formed.

In Fig. 2, the amount of charge of dust particles within given radius r is compared with that of the background charge as functions of $(r/a)^3$ in some cases including those shown in Fig. 1: When the condition of the charge neutrality is satisfied locally, these two would coincide with each other. We observe that, with the increase of the temperature, dust particles become distributed with increased uniformity and the condition of charge neutrality is satisfied increasingly more locally. With the decrease of the temperature, in contrast, we have sharper boundary of distribution and eventually some shells are formed.

C. Experimental formulas for shell structures

We here summarize some observations on low temperature shell structures obtained by molecular dynamics. Our

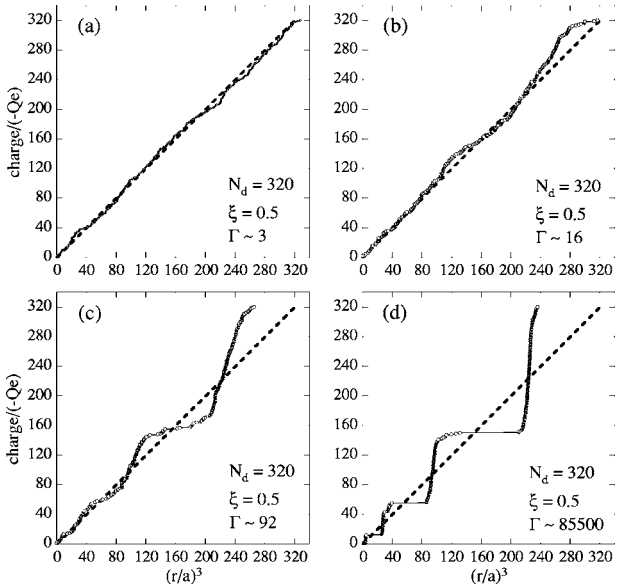

FIG. 2. The amount of charge carried by particles within radius r normalized by $-Qe$. Dotted lines are that of background charge normalized by Qe.

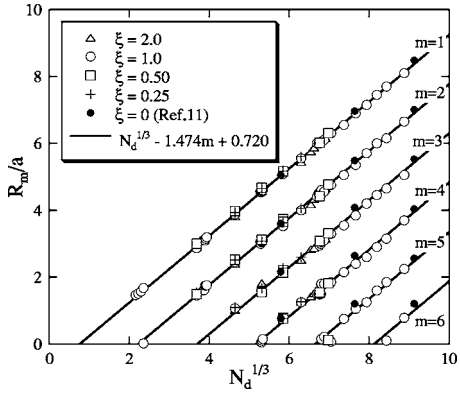

FIG. 3. Positions of shells. Different symbols are the results for different values of ξ. Solid lines are values given by an interpolation.

main interest will be in their dependency on N_d and ξ in the domain of relatively large N_d.

With the increase of the number of dust particles N_d, the positions of shells move outwards and a new shell appears at the center one by one when N_d exceeds each critical value. We number the shells as 1, 2,…, from outside to inside and denote the radius of the mth shell by R_m. In Fig. 3 we plot the values of R_m normalized by a, $R'_m=R_m/a$, for several values of ξ as functions of $N_d^{1/3}$. We include also the result for the pure Coulombic case of $\xi=0$ [10,11] from [11].

We observe that R'_m increases in proportion to $N_d^{1/3}$ and the structure as a whole is almost independent of the strength of screening ξ. This indicates that the local configuration of particles is characterized by a unique length, the mean distance a, throughout the sphere. These results are consistent with and extend our previous observation that the critical values of N_d for the transition of structure (increase of shell number) have no systematic dependence on ξ [7]. Based on this observation, we assume that the structure does not depend on the value of ξ in what follows.

We further find that the constant of proportionality of the increment of R'_m to that of $N_d^{1/3}$ is almost unity. We may thus write with sufficient accuracy

$$R'_m(N_d) = R_m(N_d)/a = N_d^{1/3} - N_{d,m}^{1/3} \quad (N_d \geqslant N_{d,m}), \quad (3.4)$$

where $N_{d,m}$ is the critical value of N_d for the appearance of the mth shell. We interpolate our data for R'_m by the formula (3.4) as shown in Fig. 3 by solid lines and determine the critical values $N_{d,m}$ as given in Table I and plotted in Fig. 4. We see that these critical values are approximately expressed as $N_{d,m}^{1/3}=a_1 m+a_2$. When fitted to the above formula, the results in Table I give $a_1=1.474$ and $a_2=-0.720$. We thus have

TABLE I. Critical values of $N_d^{1/3}$, $N_{d,m}^{1/3}$, for the appearance of the shell m.

m	1	2	3	4	5	6
$N_{d,m}^{1/3}$	0.713	2.235	3.743	5.208	6.627	8.099

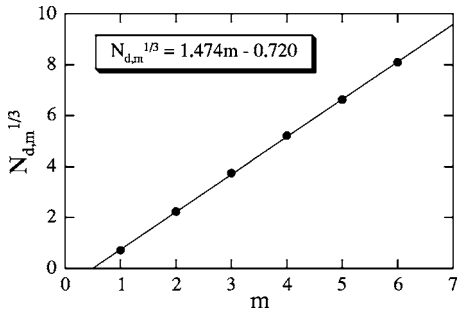

FIG. 4. Critical values for the appearance of the shell m. Solid line is an interpolation.

$$N_{d,m}^{1/3} = 1.474m - 0.720 \tag{3.5}$$

or

$$R'_m(N_d) = R_m(N_d)/a = N_d^{1/3} - 1.474m + 0.720 \quad (N_d \geqslant 1.474m - 0.720). \tag{3.6}$$

It should be noted that the linear dependence of $N_{d,m}^{1/3}$ on m corresponds to an equal spacing for shells.

The populations on shells N_m are plotted in Fig. 5. We may expect that they are proportional to $4\pi\sigma_m R_m^2$ where σ_m is the surface density on the shell m. In the light of Eq. (3.4), we interpolate the results given in Fig. 5 by the form

$$N_m = 4\pi\sigma_m a^2 (N_d^{1/3} - N_{d,m}^{1/3})^2, \tag{3.7}$$

where $\sigma_m a^2$ is the normalized surface number density on the shell m. Interpolations are shown in Fig. 5 by solid lines and the values of $\sigma_m a^2$ are given in Table II (values given in Table I are used for $N_{d,m}$). We see that $\sigma_m a^2$ are almost independent of m, giving

$$\sigma a^2 \sim 0.356 \tag{3.8}$$

for the surface density σ (averaging over values in Table II except for the innermost shell $m=6$), and populations on shells are expressed by the formula

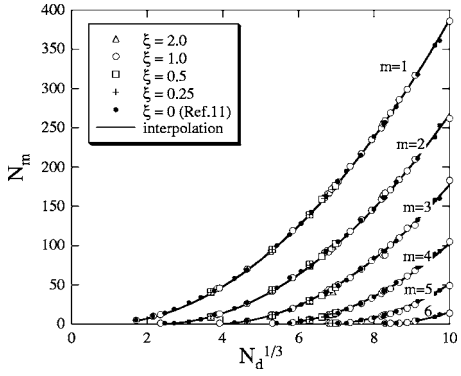

FIG. 5. Populations on shells. Solid lines are values given by an interpolation.

TABLE II. Normalized surface densities on shells $\sigma_m a^2$.

m	1	2	3	4	5	6
$\sigma_m a^2$	0.361	0.352	0.356	0.352	0.361	0.342

$$N_m = 4\pi \times 0.356 (N_d^{1/3} - N_{d,m}^{1/3})^2 = 4.48 (N_d^{1/3} - N_{d,m}^{1/3})^2, \tag{3.9}$$

to a good accuracy.

D. An interpretation based on close-packed structures

We here try to interpret the results of simulation based on a simple consideration. We first note that the charge carried by each shell is balanced by background charge which surrounds the corresponding shell from both inside and outside. The background charge between two shells of radii R_m and R_{m+1}, for example, may thus be divided at the halfway into the one responsible for the shell m and the one for the shell $m+1$. Since the distribution of the background charge is a sphere of radius R, the radius of the outermost shell R_1 is then smaller than R by approximately half of the shell spacing. Assuming the equality of the shell spacing and denoting the latter by d, we may have

$$R_1(N_d) = R - 0.5d. \tag{3.10}$$

Since $R/a = N_d^{1/3}$ due to Eq. (3.3), this is rewritten as

$$\frac{R_1(N_d)}{a} = N_d^{1/3} - 0.5\frac{d}{a} \tag{3.11}$$

and for inner shells, we have

$$\frac{R_m(N_d)}{a} = N_d^{1/3} - \frac{d}{a}(m - 0.5). \tag{3.12}$$

Comparing the result (3.12) with the simulation (3.6) which is rewritten as

$$R'_m(N_d) = N_d^{1/3} - 1.474\left(m - \frac{0.720}{1.474}\right) = N_d^{1/3} - 1.474(m - 0.488), \tag{3.13}$$

we may have

$$\frac{d}{a} \sim 1.47 \tag{3.14}$$

with the accuracy indicated by a small difference $0.5 - 0.488 = 0.012$ which may justify our consideration leading to Eq. (3.12).

It is interesting to note that this spacing between shells is close to the spacing of triangular lattice plane in the closest-packed structure. In both the face-centered-cubic (fcc) and the hexagonal-close-packed (hcp) structure, the spacing between stacked plane (ABCABC… for fcc and ABAB… for hcp) is given by $1.477a$. This spacing gives

$$\frac{R_m(N_d)}{a} = N_d^{1/3} - 1.477(m-0.5). \tag{3.15}$$

This may suggest that the local structure is close to these close-packed structures even in finite clusters. In fact, when plotted in Fig. 3, the expression (3.15) above is almost indistinguishable from Eq. (3.6). The surface density on these lattice planes σ_{close} is calculated to be

$$\sigma_{close}a^2 = \frac{3^{1/6}}{(2\pi)^{2/3}} = 0.3527 \tag{3.16}$$

which is close to the value in Eq. (3.8), 0.356, given by simulations.

In the case of Coulombic particles, the structure of the bulk ground state takes over the shell structure as the ground state of clusters when the number of particles exceeds the critical size $N_c \sim (1.1-1.5)\times 10^4$ [12]. The critical value for Yukawa clusters is not known and, as far as the system sizes simulated here, the ground state is given by the shell structure.

IV. SHELL MODEL

In this section, we apply the shell model which has been successful in reproducing the ordered structures in ion traps with cylindrical symmetry [13] and in dust particles under one-dimensional confinement due to gravity [2,3].

A. Without cohesive energy

We start from the assumption that dust particles are organized into thin spherical shells and minimize the total energy of the system with respect to parameters determining the structure, the number of shells N_{shell}, shell radii R_m $(m=1,2,\ldots,N_{shell})$, and the shell populations N_m $(m=1,2,\ldots,N_{shell})$, under the condition

$$\sum_{m=1}^{N_{shell}} N_m = N_d. \tag{4.1}$$

We first note that the potential field of a shell of radius R_i with a population N_i is given by

$$\phi_i(r) = \int d\mathbf{r}' \frac{\exp(-|\mathbf{r}-\mathbf{r}'|/\lambda)}{|\mathbf{r}-\mathbf{r}'|} \frac{N_i}{4\pi R_i^2} Qe\,\delta(r'-R_i) \tag{4.2}$$

and calculated as

$$\phi_i(r) = \frac{1}{2}\frac{\lambda}{r}\frac{N_i}{R_i} Qe\{\exp(-|r-R_i|/\lambda) - \exp[-(r+R_i)/\lambda]\}. \tag{4.3}$$

The interaction between the shell i and the shell j is thus given by

$$(Qe)N_j\phi_i(R_j) = \frac{1}{2}(Qe)^2\frac{\lambda N_i N_j}{R_i R_j}\{\exp(-|R_i-R_j|/\lambda) - \exp[-(R_i+R_j)/\lambda]\} \tag{4.4}$$

and the total interaction energy per particle is written as

$$\Psi_{int} = \frac{(Qe)}{2N_d}\sum_{i,j}^{N_{shell}} N_j\phi_i(R_j) = \frac{(Qe)^2}{4N_d}\sum_{i,j}^{N_{shell}} \frac{\lambda N_i N_j}{R_i R_j} \times\{\exp(-|R_i-R_j|/\lambda) - \exp[-(R_i+R_j)/\lambda]\}. \tag{4.5}$$

Including the energy due to the confining potential

$$\Psi_{ext} = \frac{1}{N_d}\sum_{i=1}^{N_{shell}} N_i\phi_{ext}(R_i), \tag{4.6}$$

we have the total energy per particle $\Psi_{int}+\Psi_{ext}$.

When $\Psi_{int}+\Psi_{ext}$ is minimized with respect to N_{shell}, R_m, and N_m, we have the optimized structure given by infinite number of shells or $N_{shell}\to\infty$ and $N_m\to 0$. As is shown in previous analyses, it is thus essential in our shell model to take the cohesive (interaction) energy within the shell into account [2,13].

B. With cohesive energy

Since particles are in an ordered state of a triangular lattice with defects on each shell, they have lower energy compared with the state of random configuration (uniform distribution) on a sphere. We approximate this gain (cohesive energy) per particle by that of a two-dimensional Yukawa lattice which is expressed by a dimensionless function e_{coh} as $(Qe)^2(\pi n_s)^{1/2}e_{coh}[1/\lambda(\pi n_s)^{1/2}]$. Here n_s is the surface density and e_{coh} is interpolated as [3,14]

$$e_{coh}(x) = -1.9605 + 0.8930x - 0.1959x^2 + 0.01715x^3. \tag{4.7}$$

The cohesive energy is then given by

$$\Psi_{coh} = \frac{(Qe)^2}{N_d}\sum_{i=1}^{N_{shell}} N_i(\pi n_i)^{1/2}e_{coh}[1/\lambda(\pi n_i)^{1/2}], \tag{4.8}$$

where $n_i = N_i/4\pi R_i^2$ is the surface density on the shell i.

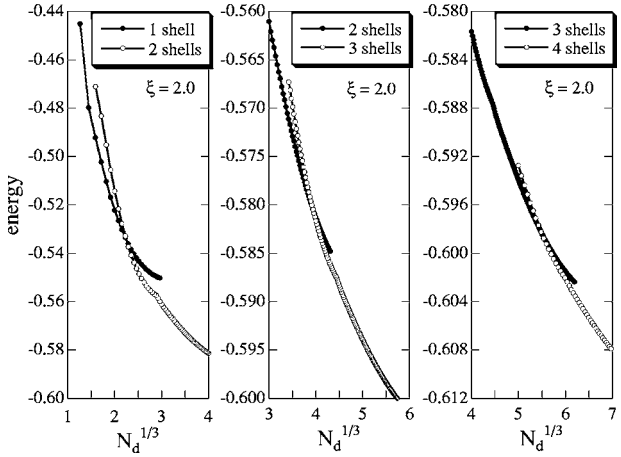

FIG. 6. Minimum of $\Psi_{int}+\Psi_{ext}+\Psi_{coh}$ in the unit of $(Qe)^2/a$ optimized for $\{R_m,N_m\}_{m=1,2,\ldots,N_{shell}}$ for given values of N_{shell}. With increasing N_d, the number of shells changes from one to two, from two to three, and from three to four, when these lines cross.

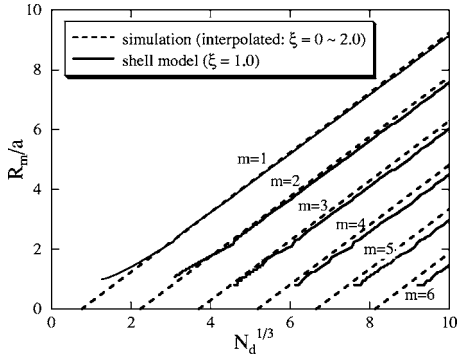

FIG. 7. Positions of shells. Solid lines are values given by the shell model. Dotted lines are results of simulations expressed by an interpolation.

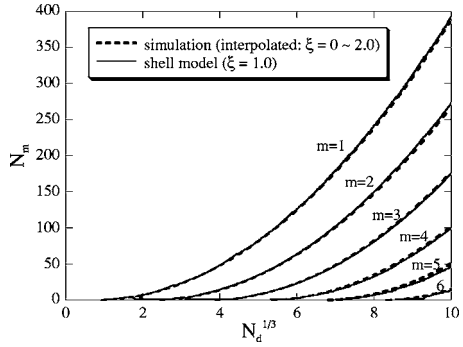

FIG. 8. Populations on shells. Solid lines are values given by shell model. Dotted lines are results of simulations expressed by an interpolation.

When $\Psi_{int}+\Psi_{ext}+\Psi_{coh}$ is minimized with respect to $\{R_m,N_m\}_{m=1,2,\ldots,N_{shell}}$ for given N_{shell}, we have the results as typically shown in Fig. 6 where optimized values of $\Psi_{int}+\Psi_{ext}+\Psi_{coh}$ are plotted in the unit of $(Qe)^2/a$ as functions of N_d: When these lines cross, the number of shells corresponding to the global minimum changes. We observe that, with the increase of N_d, the optimum value of the total energy is realized with increasing N_{shell}. We also note that the results are almost independent of the value of ξ for $0<\xi<2$.

We plot the resultant positions and populations of shells in Figs. 7 and 8, respectively, in comparison with those of simulations given by the interpolations (3.6) and (3.9). As for the positions of shells shown in Fig. 7, our model gives somewhat smaller radii for inner shells. This may be due to our applying the cohesive energy of the planar system to spherical shells. The overall agreement with simulation is satisfactory and we may conclude that our model reproduces the number, positions, and populations of shells to a good accuracy as in previous cases [2,13].

V. CONCLUSIONS

We have analyzed the structure of spherical clusters of Yukawa particles by numerical simulations and theoretical approaches. Dust particles in dusty plasmas can be regarded as interacting via Yukawa interaction and such spherical structures appear in the isotropic environment realized under microgravity [4,5] or by active cancellation of the effect of gravity [6].

We have first shown that the condition of the overall charge neutrality in dusty plasmas leads to an effective external confining potential for Yukawa particles representing dust particles. Assuming the isotropy of the system, we have observed the appearance of spherical shells at low temperatures. When scaled by the mean distance, the structure is almost independent of the strength of screening and shells have approximately equal spacing which corresponds to that of lattice planes in close-packed structures. Extending the shell model and including the cohesive energy within each sphere, we have shown that the structure can be reproduced to a good accuracy.

Since the Yukawa potential covers both the long-ranged and short-ranged interactions, these results will be useful as an example of three-dimensional finite systems of confined particles with repulsive interaction. They may also serve as a reference in the cases where the isotropy of environment is not realized completely.

[1] J. H. Chu and Lin I, Physica A **205**, 183 (1994); Phys. Rev. Lett. **72**, 4009 (1994); H. Thomas, G. E. Morfill, V. Demmel, J. Goree, B. Feuerbacher, and D. Mohlmann, *ibid.* **73**, 652 (1994); Y. Hayashi and K. Tachibana, Jpn. J. Appl. Phys., Part 2 **33**, L804 (1994); A. Melzer, T. Trottenberg, and A. Piel, Phys. Lett. A **191**, 301 (1994).

[2] H. Totsuji, T. Kishimoto, and C. Totsuji, Phys. Rev. Lett. **78**, 3113 (1997).

[3] H. Totsuji, T. Kishimoto, and C. Totsuji, Jpn. J. Appl. Phys., Part 1 **36**, 4980 (1997).

[4] G. E. Morfill, H. M. Thomas, U. Konopka, H. Rothermel, M. Zuzic, A. Ivlev, and J. Goree, Phys. Rev. Lett. **83**, 1598 (1999).

[5] V. E. Fortov, O. S. Vaulina, O. F. Petrov, V. I. Molotkov, A. M. Lipaev, V. M. Torchinsky, H. M. Thomas, G. E. Morfill, S. A. Khrapak, Yu. P. Semenov, A. I. Ivanov, S. K. Krikalev, A. Yu. Kalery, S. V. Zaletin, and Yu. P. Gidzenko, Phys. Rev. Lett. **90**, 245005 (2003).

[6] O. Arp, D. Block, A. Piel, and A. Melzer, Phys. Rev. Lett. **93**, 165004 (2004).

[7] H. Totsuji, C. Totsuji, T. Ogawa, and K. Tsuruta, Phys. Rev. E **71**, 045401(R) (2005).

[8] S. Hamaguchi and R. T. Farouki, J. Chem. Phys. **101**, 9876 (1994).

[9] Y. Rosenfeld, Phys. Rev. E **49**, 4425 (1994).

[10] D. H. E. Dubin and T. M. O'Neil, Phys. Rev. Lett. **60**, 511 (1988).

[11] R. W. Hasse and V. V. Avilov, Phys. Rev. A **44**, 4506 (1991).

[12] H. Totsuji, T. Kishimoto, C. Totsuji, and K. Tsuruta, Phys. Rev. Lett. **88**, 125002 (2002).

[13] H. Totsuji and J.-L. Barrat, Phys. Rev. Lett. **60**, 2484 (1988).

[14] C. Totsuji, M. S. Liman, K. Tsuruta, and H. Totsuji, Phys. Rev. E **68**, 017401 (2003).